ACS APPLIED MATERIALS & INTERFACES

Research Article

www.acsami.org

Pulsed Laser-Deposited MoS_2 Thin Films on W and Si: Field Emission and Photoresponse Studies

Dattatray J. Late,*[,†,‡] Parvez A. Shaikh,[†] Ruchita Khare,[§] Ranjit V. Kashid,[§] Minakshi Chaudhary,[†] Mahendra A. More,[§] and Satishchandra B. Ogale*[,†,‡]

[†]Physical & Materials Chemistry Division, CSIR-National Chemical Laboratory, Dr. Homi Bhabha Road, Pune 411008, India

[‡]Academy of Scientific and Innovative Research, Anusandhan Bhawan, Rafi Marg, New Delhi 110001, India

[§]Center for Advanced Studies in Material Science and Condensed Matter Physics, Department of Physics, University of Pune, Pune 411007, India

Supporting Information

ABSTRACT: We report field electron emission investigations on pulsed laser-deposited molybdenum disulfide (MoS_2) thin films on W-tip and Si substrates. In both cases, under the chosen growth conditions, the dry process of pulsed laser deposition (PLD) is seen to render a dense nanostructured morphology of MoS_2, which is important for local electric field enhancement in field emission application. In the case of the MoS_2 film on silicon (Si), the turn-on field required to draw an emission current density of 10 $\mu A/cm^2$ is found to be 2.8 V/μm. Interestingly, the MoS_2 film on a tungsten (W) tip emitter delivers a large emission current density of ~30 mA/cm^2 at a relatively lower applied voltage of ~3.8 kV. Thus, the PLD-MoS_2 can be utilized for various field emission-based applications. We also report our results of photodiode-like behavior in (n- and p- type) Si/PLD-MoS_2 heterostructures. Finally we show that MoS_2 films deposited on flexible kapton substrate show a good photoresponse and recovery. Our investigations thus hold great promise for the development of PLD MoS_2 films in application domains such as field emitters and heterostructures for novel nanoelectronic devices.

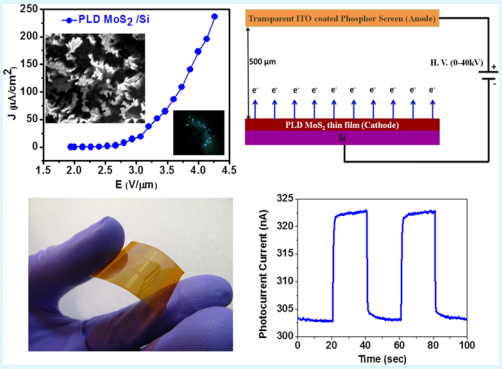

KEYWORDS: *MoS_2, pulsed laser deposition, thin film, field emission, photodiode heterostructures*

1. INTRODUCTION

Field-emission display (FED) devices contain nanotip structures that emit electrons under the application of a strong electrostatic field (10^6–10^7 V/cm), and these electrons accelerated by a few kilovolt potential generate an image on a phosphor screen via cathodoluminescence. The FEDs provide high contrast and brightness along with good picture quality at low power consumption, as compared to other displays. Currently, most of the field emission-based devices use an array of micro/nanotips as a cathode (termed as Spindt cathode), which essentially requires e-beam lithography or photolithography for fabrication purposes. In contrast to the Spindt cathodes, a cheaper and simpler alternative can be an unpatterned thin film(s) of high aspect ratio nanostructures (termed as a planar cathode). In addition to display devices, one of the application domains for cold cathodes is the electron microscope, wherein "point" source geometry (similar to a conventional single microtip cathode) is desirable, rather than a planar cathode.[1] For fabrication of field emission-based electron sources, various one-dimensional (1D) and two-dimensional (2D) nanomaterials such as carbon nanotubes,[2−4] zinc oxide,[5−8] tin oxide,[9,10] graphene,[11,12] MoS_2 nanotubes[13] and nanoflowers,[14] lanthanum hexaboride thin films[15−18] etc., have been widely explored. Currently, 2D atomically thin inorganic layered materials are being considered as potential candidates for planar device technologies and very recently have been investigated by a number of researchers.[19−36]

Among the various inorganic 2D layered materials, MoS_2 has attracted a great deal of attention from the scientific community in view of its unique combination of application-worthy physical properties. The structure of MoS_2 involves recurring units of layers composed of an atomic plane of Mo sandwiched between two atomic planes of S in a trigonal arrangement (S−Mo−S). Bulk MoS_2 has an indirect band gap of 1.2 eV, while atomic thin layer MoS_2 has a direct band gap of ~1.8 eV. Furthermore, MoS_2 exhibits a good electrical conductivity (~0.5 Ω^{-1} cm^{-1}).[37] Recently we have reported field emission characteristics of MoS_2 nanosheets drop casted on Si substrate, and the results are promising.[25] Such drop-casted films using presynthesized MoS_2 flakes are however fairly nonuniform due to the tendency of nanoflakes to agglomerate on the Si substrate during drying.[25] Furthermore, it was realized that

Received: June 2, 2014
Accepted: August 20, 2014
Published: August 20, 2014

these drop-casted films exhibit poor adherence to the Si substrate thereby posing a limitation for practical applications. Hence, it is desirable to explore processes for growth of nearly stoichiometric dense and well adherent films preferably via a dry processing route. PLD is one such technique that can render fairly stoichiometric transfer of atomic species from a bulk target to a thin film under controlled ambient conditions for a diverse classes of systems.[38−44] The chemical composition, resultant stoichiometry, and morphology of the PLD film depend on process variables such as laser fluence, deposition temperature, ambient type, gas pressure, etc., which can be tuned/optimized to obtain films of desired quality.[42−44] Another unique advantage offered by the PLD process is evolution of the film through surface impingement of highly energetic (0.1−10 eV) ionic and ionized radical species, as against a simple soft landing of atomic species rendered by thermal evaporation. Importantly, this ion bombardment can also assist film texture development under optimized conditions. In the context of field enhancement, such texturing clearly holds the key. Moreover, PLD being a single target process, adjusting stoichiometry is much easier than multiple source thermal evaporation or the sputtering process. Therefore, in this work we have explored the use of the PLD technique to grow MoS_2 films on Si, W, and flexible kapton substrate for evaluation of their field emission and photoresponse properties. As our results reveal, the PLD of MoS_2 films indeed renders the desirable dense nanostructured morphology of interest to field emission, yielding large emission current density with impressive field enhancement factors.[14,25] Further, the PLD MoS_2 films on flexible kapton substrates have greater prospects for flexible smart devices such as photodetectors, transistors, sensors, etc.

2. RESULTS AND DISCUSSION

The morphology of PLD MoS_2 films on Si and W-tip substrates observed using field emission scanning electron microscopy (FESEM) is depicted in Figure 1. In the case of MoS_2/W-tip sample, as seen from Figure 1a,b, the W-tip substrate surface is fully covered by the MoS_2 film, along with an overgrowth of 20−60 nm size nanocrystals of MoS_2. This reflects Stransky−Krastinov growth mode for this film−substrate combination,[39−41] which is in fact beneficial in the context of electron emitter application. The inset of Figure 1a shows the image of a bare W-tip. The surface morphology of the MoS_2/Si sample (Figure 1c) is characterized by the presence of nanometric protrusions on MoS_2 film, which uniformly covers the entire Si substrate surface.

The Raman analysis, discussed in a later section, reveals that the PLD process of MoS_2 on the W-tip and Si surfaces indeed leads to nearly stoichiometric growth of the right phase of MoS_2, because they do not show any additional features other than those observed for high quality MoS_2. X-ray photoelectron spectroscopy (XPS) analysis, presented and discussed in Supporting Information, further confirms nearly stoichiometric growth of the MoS_2 phase. Herein the word "nearly stoichiometric" implies that the atomic ratio Mo:S is fairly close to 1:2. Using atomic force microscopy (AFM), the average thickness of MoS_2 film deposited on Si substrate was estimated to be ∼120 nm.

Figure 2a shows the FESEM image of MoS_2 thin film on the Si substrate. The film surface morphology clearly shows surface protrusions which can serve the function of self-formed emitter tips. We also performed a scanning tunneling microscopy

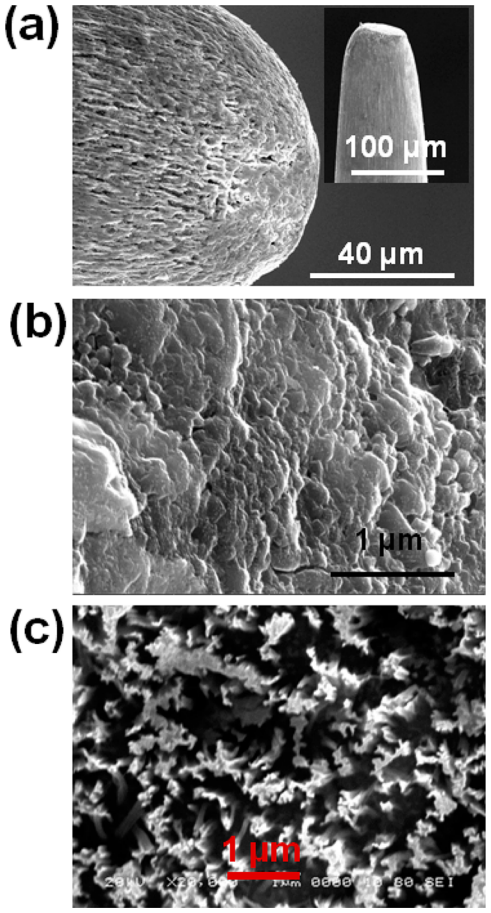

Figure 1. Field emission scanning electron microscope images of pulsed laser-deposited MoS_2 thin film: (a and b) on W-tip substrate, and (c) on Si substrate (deposited with laser fluence 2 J/cm^2, laser shots 900, thickness ∼120 nm). Inset of panel a shows an image of the bare W-tip.

(STM) study mainly to establish the n-type character of MoS_2 through tunneling measurement. For this study, the film was deposited at a lower laser energy density of 0.5 J/cm^2 with 900 shots so as to get a smoother surface. The Raman data for this film also confirmed the MoS_2 character. Figure 2b shows a typical current−voltage (I−V) characteristic of MoS_2 thin film deposited on p-Si substrate recorded using scanning tunneling spectroscopy (STS). In the inset of Figure 2b we show the I−V characteristic of p-type bare Si substrate. Note that we have only used p-type Si substrate for the scanning tunneling microscopy/spectroscopy (STM/STS) study. Further, we have also measured I−V characteristics on bare p-type Si and then the same Si substrate was used for the deposition of MoS_2 film. We calculated the bandgap of p-type Si substrate from the first derivative of I−V characteristics (inset of Figure 2b) obtained from STS data and which is observed to be 1.1 eV. The variation observed in the I−V characteristics of bare p-type Si and MoS_2 film deposited on p-type Si suggests the uniform coverage of MoS_2 thin film on p-type Si substrates.

Raman spectroscopy is a powerful technique sensitive to thickness, crystallographic orientation, stress, chemical composition, and phase transition of the material subjected to investigation. Figure 2c shows comparative Raman spectra of MoS_2 bulk and PLD MoS_2/Si emitter. Interestingly, both samples exhibit characteristic peaks corresponding to E^1_{2g} and A_{1g} modes, originating from the in-plane and out-of-plane

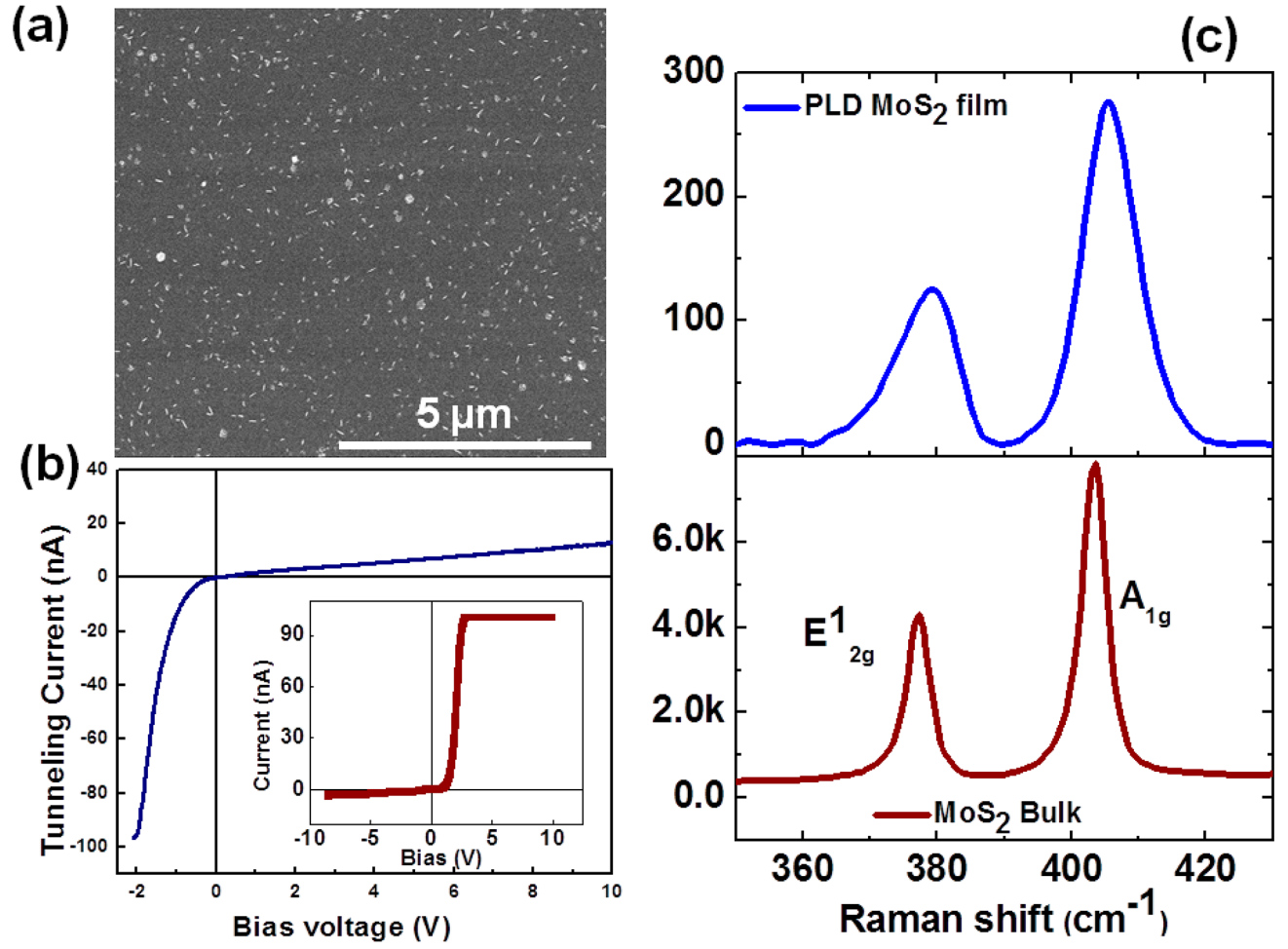

Figure 2. PLD MoS_2 thin film on Si substrate (laser fluence 0.5 J/cm^2, laser shots 900, thickness ~50 nm): (a) FESEM image. (b) Typical $I-V$ characteristics of MoS_2 thin film deposited on p-type Si, and inset of panel b shows the $I-V$ characteristic of bare p-type Si recorded using scanning tunneling spectroscopy. (c) Comparative Raman spectra of bulk MoS_2 and pulsed laser-deposited MoS_2 thin film on Si substrates.

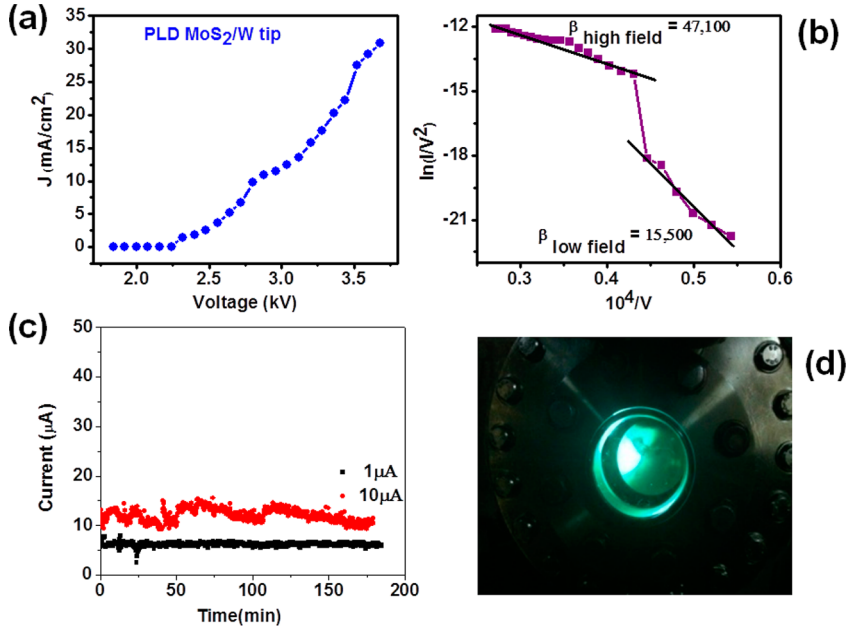

Figure 3. Field emission of PLD MoS_2 films on W-tip substrates (thickness ~120 nm): (a) $J-V$ characteristics, (b) $F-N$ plot showing nonlinear behavior indicating the emission current from the semiconducting emitter. (c) Field emission current stability ($I-t$) plot for MoS_2/W-tip emitter. (d) Field emission image recorded at 3.2 kV.

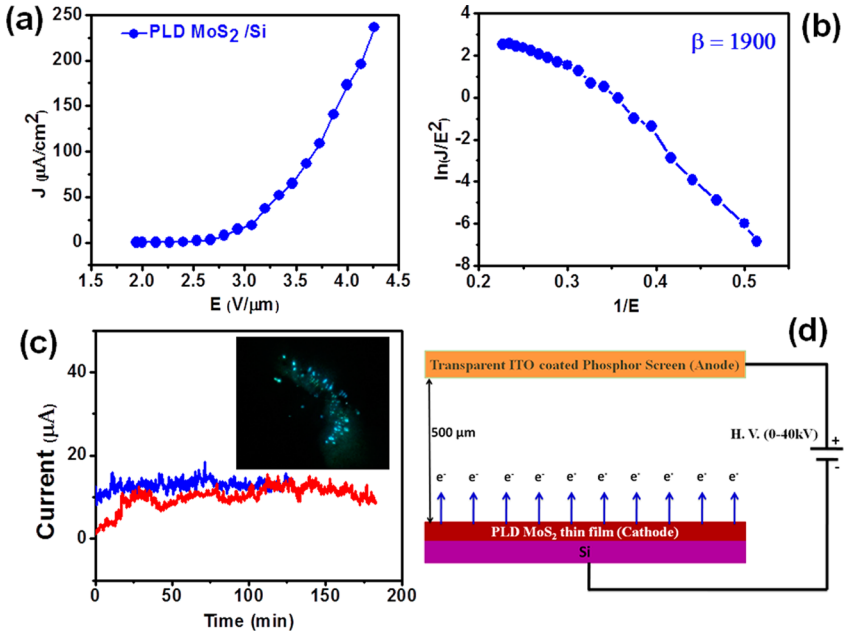

Figure 4. Field emission of PLD MoS_2 thin film on Si substrates (thickness ~120 nm). (a) $J-E$ characteristics, (b) $F-N$ plot $\ln(J/E^2)$ vs $1/E$, (c) field emission current stability ($I-t$) plot, and (d) field emission setup used for field emission investigations of PLD MoS_2/Si. Inset of panel c shows the field emission image recorded at an applied electric field of 3.5 V/μm.

vibrations, respectively. Furthermore, the Raman data reveal broadening and phonon shifts in both the E^1_{2g} and A_{1g} modes. The observed spectra of bulk sample as well as pulsed laser-deposited thin film samples were attributed to MoS_2. Our Raman results are found to be consistent with the reported results in the literature.[19,45−47]

The FE measurements were carried out on PLD MoS_2 thin film on planar Si and W-tip substrates. The advantage of using MoS_2 thin films, for planner device technology such as flat panel field emission display, and W-tips offers many opportunities for both fundamental research and practical applications such as field emission display and an intense "point" electron source, respectively.

Figure 3a shows the field emission current density (J) versus applied voltage (V) graph of the MoS_2/W-tip field emitter. With the gradual increase in applied voltage, the emission current increases rapidly, indicating that the emission is indeed as per the Fowler−Nordheim ($F-N$) theory.[48−50] It is interesting to note that we could draw emission current density as large as 30 mA/cm^2 at an applied voltage of 3.8 kV. The observed $J-V$ characteristics are further analyzed by plotting a graph of $\ln(I/V^2)$ versus $(10^4/V)$, known as a $F-N$ plot. Figure 3b represents the corresponding $F-N$ plot, which exhibits nonlinear nature over the entire field range. The nonlinearity observed in the $F-N$ plot is a direct consequence of the semiconducting nature of MoS_2. On the basis of the theory of field electron emission from semiconductors, the low electric field region corresponds to the electron emission from the conduction band, while the high electric field region corresponds to the electron emission from the conduction band and the valence band of MoS_2.

Modifications to the original $F-N$ theory for different semiconducting materials have been discussed in the literature.[48−50] A modified $F-N$ equation[48−50] is used for the analysis of field emission current density versus applied electric field data from the $F-N$ plot for PLD MoS_2 thin film. The modified $F-N$ equation is as follows,

$$J = \lambda_M a\varphi^{-1}E^2\beta^2 \exp\left(-\frac{b\varphi^{3/2}}{\beta E}\upsilon_F\right)... \quad (1)$$

where λ_M is the macroscopic pre-exponential correction factor, J is the emission current density, E is the applied average electric field (surface field), a and b are the constants (a = 1.54 × 10^{-6} AeV/V^2, b = 6.83 eV$^{-3/2}$ Vnm^{-1}), φ is the work funtion of the emitter, β is the field enhancement factor, and υ_F (correction factor) is a particular value of the principal Schottky−Nordheim barrier function υ. The field enhancement factor is calculated from the slope (m) of $F-N$ plot and work function of the emitter. According to the modified $F-N$ theory,[48−50] β is expressed as,

$$\beta = \frac{(-6.8 \times 10^3)\varphi^{3/2}}{m} \quad (2)$$

Due to the presence of sharp protrusions on the emitter surface, the local electric field at the apex of such protrusions becomes amplified/enhanced and the corresponding field enhancement factor (β) can be estimated using eq 2. In the present case, to determine the value of the slope (m), the observed $F-N$ plot is resolved into two linear sections in low and high field regions. By taking the value of φ for MoS_2 as 4.36 eV[51,52] the values of β are estimated to be ~15 500 and ~47 000 corresponding to the low and high field regions of MoS_2 film deposited on W-tip substrate. Indeed such high values of β are due to the presence of sharp nanometric size protrusions on the emitter surface.

Figure 3c depicts the FE current stability characteristics of the PLD MoS_2/W-tip emitter, investigated at preset values of 1 μA and 10 μA, over a period of 3 h. The emitter exhibits good emission current stability at a preset value of ~1 μA. At a higher preset value (10 μA), the emission stability curve exhibits "excursions". Furthermore, a careful observation reveals that the excursions are superimposed with "spikes". The main cause of "spike"-like fluctuations are the adsorption/desorption and ion

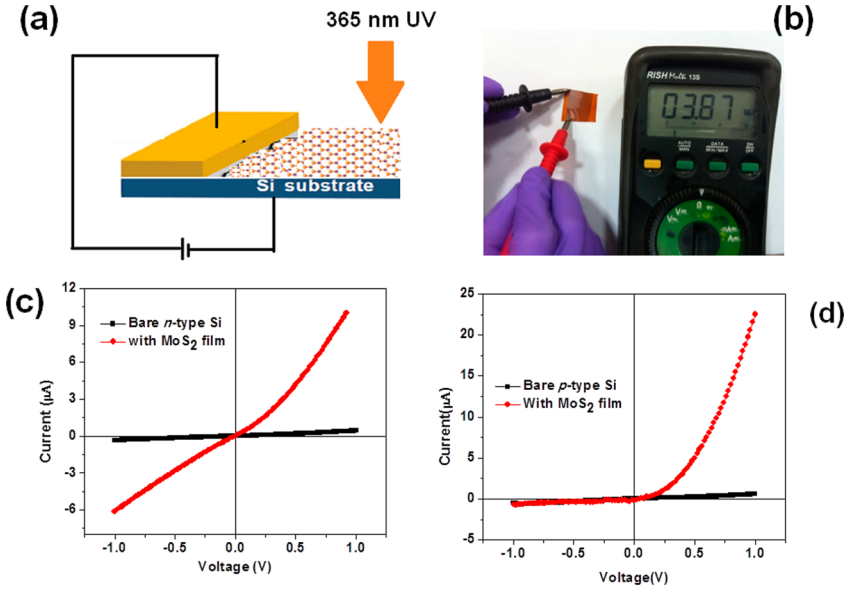

Figure 5. (a) Schematic of MoS_2−Si heterostructure device. (b) PLD MoS_2 film deposited on flexible plastic kapton substrates shows conducting behavior. (c) *I*−*V* curves of n-Si/MoS_2 heterostructures (thickness ∼30 nm) upon light illumination of wavelength 365 nm and +1 V bias. (d) *I*−*V* curves of p-Si/MoS_2 heterostructures (thickness ∼30 nm) upon light illumination of wavelength 365 nm and +1 V bias.

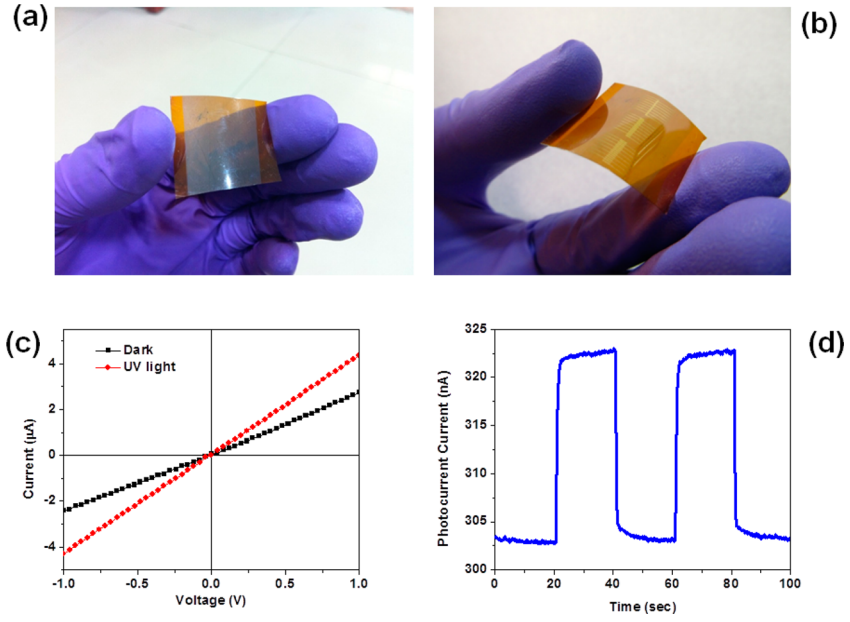

Figure 6. (a) PLD MoS_2 film (thickness ∼30 nm) deposited on flexible plastic kapton substrate can be clearly visible under white light. (b) Typical gold electrode pattern on PLD MoS_2/flexible plastic kapton substrate (c) *I*−*V* curves of MoS_2 upon light illumination wavelength of 365 nm and +1 V bias. (d) Photoresponse of PLD MoS_2 film on flexible plastic kapton substrate without any bias.

bombardment of residual gas molecules.[11−18] During adsorption/desorption events, the local work function of the MoS_2 thin film emitter varies slightly depending upon the nature of the adsorbing molecule (either electropositive/electronegative on the MoS_2 emitter surface). Also, ion bombardment of residual gas molecules due to the presence of a high electrostatic field may lead to mechanical damage, creating and destroying the emission sites at the MoS_2 thin film surface, which in turn cause the fluctuations in the field emission current. Figure 3d shows the field emission image of the PLD MoS_2/W-tip emitter depicting the number of emission sites representative of the presence of nanometric sharp protrusions on the emitter surface. Postfield emission SEM investigations were also carried out on the MoS_2/W-tip emitter which revealed no severe deterioration of the emitter surface after long-term operation. This clearly signifies that the MoS_2 thin film prepared using PLD has excellent adhesion with the substrate.

The *J*−*E* plot for the PLD MoS_2/Si planar emitter is shown in Figure 4a. The turn-on field required to draw emission current density of 1 $\mu A/cm^2$ is observed to be 2 V/μm. This value of the electric field corresponding to 10 $\mu A/cm^2$ is found to be 2.8 V/μm, which is lower than that reported for a few layers of MoS_2 nanosheet/Si emitter (∼3.5 V/μm).[25] The low turn-on field observed in the present case may be attributed to the presence of sharp protrusions and better electrical contact

dx.doi.org/10.1021/am503464h | ACS Appl. Mater. Interfaces 2014, 6, 15881−15888

between the emitter (MoS_2) and substrate surface, anticipated during PLD. It can be speculated that during film growth, the substrate surface experiences bombardment from high energetic ionic/radical species, which facilitates better electrical contact. Figure 4b shows the $F-N$ plot for the PLD MoS_2/Si planar emitter. The observed linear nature of the $F-N$ plot indicates that the field emission from the PLD MoS_2 thin film on Si substrate follows the quantum mechanical tunneling process.[48−50] The field enhancement factor (β) calculated from eq 2 was found to be ∼1900. The observed high field enhancement factor can be attributed to the presence of nanometric size protruding emitters of MoS_2 (as evidenced by the FESEM image Figure 1c). These nanometric size protrusions, offering a high field enhancement factor, are mainly responsible for the observed low turn-on field value. Figure 4c shows the emission current−time ($I-t$) behavior measured at the preset current values of 1 μA and 10 μA. The emission current fluctuations are observed to be within ±10% of average value. The inset of Figure 4c shows the field emission image of the PLD MoS_2/Si planar emitter. Figure 4d shows the typical experimental setup used for field emission investigations of PLD MoS_2/Si.

The PLD MoS_2 thin films were also deposited on p- and n-type clean Si substrates. Figure 5a shows the schematic of MoS_2−Si heterostructure, and Figure 5b shows the typical PLD MoS_2 film deposited on flexible plastic kapton substrates showing conducting behavior. We unambiguously analyzed the dependence of photoreponse behavior of PLD MoS_2 film deposited on n-type Si and p-type Si substrates with UV light wavelength of 365 nm (∼1000 mW/cm^2). Figure 5c shows the $I-V$ curves for n-Si/MoS_2 heterostructures upon UV light illumination (wavelength 365 nm) at +1 V bias, and Figure 5d shows similar $I-V$ curves for the p-Si/MoS_2 heterostructures (p-Si and n-Si resistivity ∼1−10 Ω-cm). Upon UV light illumination, the reverse photocurrent is instantly increased and reaches ∼9 μA for n-Si and ∼22 μA for p-Si substrate, which clearly indicates that the PLD MoS_2 films show a strong response to ultraviolet light in these heterostructures. Upon UV illumination, the excitons from an atomically thin layer of MoS_2 film will be generated with energy larger than the bandgap. In the case of forward bias, the photoexcited holes in the valence band do not move to n-Si because of the larger barrier and lower band offset.[53] Figure 5d shows the $I-V$ curves of p-Si/MoS_2 under UV light illumination. The $I-V$ curve clearly shows the rectifying characteristic. As seen from Figure 5, panels c and d, for the case of p-Si/MoS_2 heterostructure, photocurrent increases slowly and has no tendency to saturate, but for the case of n-Si/MoS_2 heterostructure, photocurrent increases rapidly.

Figure 6a shows the typical PLD MoS_2 film on kapton substrate (clearly visible under white light), and Figure 6b shows the typical gold electrode pattern on PLD MoS_2/flexible kapton substrate. The Au electrodes were deposited on MoS_2 film with the help of a shadow mask on flexible plastic kapton substrates. Gold was chosen as electrode material on the basis of lower contact resistance. The typical $I-V$ curve of Au/MoS_2 shows linear (ohmic) characteristics. Figure 6c shows the $I-V$ curves of MoS_2 upon light illumination wavelength of 365 nm and +1 V bias. Figure 6d shows the typical photoresponse of PLD MoS_2 film on kapton substrate without any bias voltage. The device shows a fast response and recovery of a few seconds.

3. CONCLUSIONS

Dense nanostructures of nearly stoichiometric MoS_2 were grown on Si and W-tip substrates under an optimized PLD process, and their field emission characteristics were investigated. In the case of planar MoS_2/Si emitter the value of turn-on field, required to draw current density of 10 μA/cm^2, was found to be 2.8 V/μm, which is considerably lower than the previously reported values. Interestingly, the MoS_2/W-tip emitter, due to the presence of nanometric protrusions on the surface, exhibits the capability to deliver large emission current density of ∼30 mA/cm^2 at an applied voltage of 3.8 kV. The overall FE results obtained herein are very promising and suggest that the PLD-grown MoS_2 on Si and W offers many opportunities for both fundamental research and practical applications such as field emission display and an intense "point" electron source, respectively. We also demonstrated photodiode-like behavior of (n- or p-type) Si/MoS_2 heterostructures fabricated using PLD, which is attributed to the separation of photogenerated excitons induced by the electric field at the MoS_2−Si interface. PLD MoS_2 films on flexible kapton substrate show a good UV photoresponse, which suggests that layered transition metal dichalcogenides have great potential to be used in future flexible device technology and applications.

4. EXPERIMENTAL METHODS

PLD of MoS_2 Thin Film. The MoS_2 pellet was prepared from commercial MoS_2 powder (purity of 99.95%, Aldrich Sigma Chemicals) with poly(vinyl alcohol) as a binder, applying a pressure of 75 kN/cm^2 followed by sintering under argon (Ar) atmosphere at 800 °C for 12 h. The MoS_2 pellet was then mounted on a rotating target holder at a distance of ∼5 cm from the substrates. The W-tip was prepared by using standard electrochemical polishing of a piece of W(110)-oriented wire in 1 N potassium hydroxide solution. The W-tip was mounted on a substrate holder in such a way that its apex was normal to the substrate holder base, facing toward the target. The Si and W-tip substrates were cleaned using a standard set of wafer-cleaning steps. MoS_2 thin films were deposited on the Si (n- and p-) planar, W-tip, and flexible plastic kapton substrates in a metal chamber evacuated to a base pressure of ∼5 × 10^{-5} mbar. For PLD, a pulsed krypton fluoride (KrF) excimer laser (λ = 248 nm, repetition rate 5 Hz/s, pulse width 20 ns, laser fluence ∼2 J/cm^2) was used. The deposition was carried out in Ar atmosphere at ∼1 × 10^{-2} mbar pressure. During the PLD of MoS_2 films, Si and W-tip substrates were held at a high temperature of ∼700 °C. The plastic flexible kapton substrates were kept at ∼450 °C.

Scanning Electron Microscopy (SEM). FESEM images were taken using a Nova Nano field emission (FE) SEM 450.

Raman Spectroscopy. Raman spectra on PLD MoS_2 films were recorded in backscattering geometry using a HRLabRam system with 532.5 nm as an excitation radiation, derived from an Ar ion laser of 1 mW power.

Field Emission. The field emission studies of a pulsed laser-deposited MoS_2 thin film on Si and W-tip substrates were carried out in separate experimental batches in a UHV chamber evacuated to a base pressure of ∼1 × 10^{-8} mbar. The UHV system comprises a turbomolecular pump backed by a rotary pump, a sputter ion pump, and a titanium sublimation pump. To achieve a base pressure of ∼1 × 10^{-8} mbar, the chamber was heated at 200 °C for 12 h. The field emission studies of MoS_2/Si emitter were carried out in close proximity geometry. The close proximity setup consists of a specimen (MoS_2 thin film deposited on Si substrate size ∼5 mm × 5 mm) as a cathode and a copper rod as an anode. The interelectrode separation was maintained at 500 μm using an electrically insulating alumina spacer. The field emission current (I) versus applied voltage (V) characteristic was measured using a high voltage DC power supply

(Spellman) and an electrometer (Keithley 6514). For field emission current stability studies, the emission current was fed to a computerized data acquisition system with a sampling interval of 10 s. To test reproducibility of the field emission behavior, another sample (prepared under identical experimental conditions) was mounted in the chamber. The field emission images were recorded using a digital camera (Canon SX150IS). For this, a semitransparent phosphor screen was used as an anode, which facilitated observation of the field emission image.

Conductive STM/STS Measurements. The conductive STM/STS $I-V$ measurements and imaging were carried out using an RHK Technology-100 (United States of America) STM system in ultrahigh vacuum with platinum conductive probes. For the $I-V$ measurement, the voltage sweep ranged from +10 V to −10 V by probing a single particle of MoS_2.

UV Photoresponse. UV photoresponse of MoS_2 film deposited on p-type Si and n-type Si was measured using a UV lamp with illumination wavelength of 365 nm.

■ ASSOCIATED CONTENT

Supporting Information

AFM image, height profile, XPS data, Raman spectroscopy data of PLD MoS_2 thin films, and MoS_2 field emission band diagram. This material is available free of charge via the Internet at http://pubs.acs.org.

■ AUTHOR INFORMATION

Corresponding Authors

*E-mail: sb.ogale@ncl.res.in.

*E-mail: dj.late@ncl.res.in; datta099@gmail.com.

Author Contributions

The manuscript was written through contributions of all authors. All authors have given approval to the final version of the manuscript.

Notes

The authors declare no competing financial interest.

■ ACKNOWLEDGMENTS

The authors thank Prof. C. N. R. Rao (FRS) (Director ICMS, Bangalore, India) and Prof. Vinayak P. Dravid (Director, NUANCE, Northwestern University, Evanston, IL) for support and encouragement. One of the authors, Dr. D. J. Late, thanks Department of Science and Technology (Government of India) for Ramanujan Fellowship (grant no. SR/S2/RJN-130/2012). The research work was primarily supported by NCL-MLP project grant 028626 and DST-SERB Fast-track Young Scientist Project grant no. SB/FT/CS-116/2013 and partial support by INUP IITB project sponsored by DeitY, MCIT, Government of India. S.B.O. acknowledges Indo-Australian funding under the DST-AISRF program. R.K. thanks University Grants Commission for the award of a research scholarship. P.A.S. and M.C. thank Council of Scientific and Industrial Research for a research associate fellowship.

■ REFERENCES

(1) Fursey, G. *Field Emission in Vacuum Microelectronics*, 2nd ed.; Springer US Publications: New York, 2005.

(2) Sharma, R. B.; Late, D. J.; Joag, D. S.; Govindaraj, A.; Rao, C. N. R. Field Emission Properties of Boron and Nitrogen Doped Carbon Nanotubes. *Chem. Phys. Lett.* **2006**, *428*, 102−108.

(3) D. Heer, W. A.; Châtelain, A.; Ugarte, D. A. Carbon Nanotube Field-Emission Electron Source. *Science* **1995**, *270*, 1179−1180.

(4) Ramgir, N. S.; Mulla, I. S.; Vijayamohanan, K.; Late, D. J.; Bhise, A. B.; More, M. A.; Joag, D. S. Ultralow Threshold Field Emission From a Single Multipod Structure of ZnO. *Appl. Phys. Lett.* **2006**, *88*, 042107.

(5) Banerjee, D.; Jo, S. H.; Ren, Z. F. Enhanced Field Emission of ZnO Nanowires. *Adv. Mater.* **2004**, *16*, 2028−2032.

(6) Ramgir, N. S.; Late, D. J.; Bhise, A. B.; Mulla, I. S.; More, M. A.; Joag, D. S.; Pillai, V. K. Field Emission Studies of Novel ZnO Nanostructures in High and Low Field Regions. *Nanotechnology* **2006**, *17*, 2730.

(7) Late, D. J.; Misra, P.; Singh, B. N.; Kukreja, L. M.; Joag, D. S.; More, M. A. Enhanced Field Emission From Pulsed Laser Deposited Nanocrystalline ZnO Thin Films on Re and W. *Appl. Phys. A: Mater. Sci. Process.* **2009**, *95*, 613−620.

(8) Xing, G. Z.; Fang, X. S.; Zhang, Z.; Wang, D. D.; Huang, X.; Guo, J.; Liao, L.; Zheng, Z.; Xu, H. R.; Yu, T.; Shen, Z. X.; Huan, C. H. A.; Sum, T. C.; Zhang, H.; Wu, T. Ultrathin Single-crystal ZnO Nanobelts: Ag-catalyzed Growth and Field Emission Property. *Nanotechnology* **2010**, *21*, 255701.

(9) Chen, Y. J.; Li, Q. H.; Liang, Y. X.; Wang, T. H.; Zhao, Q.; Yun, D. P. Field Emission from Long SnO_2 Nanobelt Arrays. *Appl. Phys. Lett.* **2004**, *85*, 5682.

(10) Zhang, Z.; Gao, J.; Wong, L. M.; Tao, J. G.; Liao, L.; Zheng, Z.; Xing, G. Z.; Peng, H. Y.; Yu, T.; Shen, Z. X.; Huan, C. H. A.; Wang, S. J.; Wu, T. Morphology Controlled Synthesis and a Comparative Study of the Physical Properties of SnO_2 Nanostructures: From Ultrathin Nanowires to Ultrawide Nanobelts. *Nanotechnology* **2009**, *20*, 135605.

(11) Xiao, Z.; She, J.; Deng, S.; Tang, Z.; Li, Z.; Lu, J.; Xu, N. Field Electron Emission Characteristics and Physical Mechanism of Individual Single-Layer Graphene. *ACS Nano* **2010**, *4*, 6332−6336.

(12) Palnitkar, U. A.; Kashid, R. V.; More M, A.; Joag, D. S.; Panchakarla, L. S.; Rao, C. N. R. Remarkably Low Turn on Field Emission in Undoped, Nitrogen Doped, and Boron Doped Graphene. *Appl. Phys. Lett.* **2010**, *97*, 063102.

(13) Nemanic, V.; Zumer, M.; Zajec, B.; Pahor, J.; Remskar, M.; Mrzel, A.; Panjan, P.; Mihailovic, D. Field Emission Properties of Molybdenum Disulfide Nanotubes. *Appl. Phys. Lett.* **2003**, *82*, 04573.

(14) Li, Y. B.; Bando, Y.; Golberg, D. MoS_2 Nanoflowers and Their Field Emission Properties. *Appl. Phys. Lett.* **2003**, *82*, 1962.

(15) Late, D. J.; More, M. A.; Joag, D. S.; Misra, P.; Singh, B. N.; Kukreja, L. M. Field Emission Studies on Well Adhered Pulsed Laser Deposited LaB_6 on W Tip. *Appl. Phys. Lett.* **2006**, *89*, 123510.

(16) Late, D. J.; More, M. A.; Misra, P.; Singh, B. N.; Kukreja, L. M.; Joag, D. S. Field Emission Studies of Pulsed Laser Deposited LaB_6 Films on W and Re. *Ultramicroscopy* **2007**, *107*, 825−832.

(17) Late, D. J.; Date, K. S.; More, M. A.; Misra, P.; Singh, B. N.; Kukreja, L. M.; Dharmadhikari, C. V.; Joag, D. S. Enhanced Field Emission From LaB_6 Thin Films with Nanoprotrusions Grown by Pulsed Laser Deposition on Zr foil. *Appl. Surf. Sci.* **2008**, *254*, 3601−3605.

(18) Late, D. J.; Date, K. S.; More, M. A.; Misra, P.; Singh, B. N.; Kukreja, L. M.; Dharmadhikari, C. V.; Joag, D. S. Some Aspects of Pulsed Laser Deposited Nanocrystalline LaB_6 Film: Atomic Force Microscopy, Constant Force Current Imaging and Field Emission Investigations. *Nanotechnology* **2008**, *19*, 265605.

(19) Late, D. J.; Liu, B.; Matte, H. S. S. R.; Rao, C. N. R.; Dravid, V. P. Rapid Characterization of Ultrathin Layers of Chalcogenides on SiO_2/Si Substrates. *Adv. Funct. Mater.* **2012**, *22*, 1894−1905.

(20) Matte, H. S. S. R.; Gomathi, A.; Manna, A. K.; Late, D. J.; Datta, R.; Pati, S. K.; Rao, C. N. R. MoS_2 and WS_2 Analogues of Graphene. *Angew.Chem., Int. Ed.* **2010**, *49*, 4059−4062.

(21) Rout, C. S.; Joshi, P. D.; Kashid, R. V.; Joag, D. S.; More, M. A.; Simbeck, A.; Washington, M.; Nayak, S. K.; Late, D. J. Superior Field Emission Properties of Layered WS_2-RGO Nanocomposites. *Sci. Rep.* **2013**, *3*, 3282.

(22) Radisavljevic, B.; Radenovic, A.; Brivio, J.; Giacometti, V.; Kis, A. Single-layer MoS_2 Transistors. *Nat. Nanotechnol.* **2011**, *6*, 147−150.

(23) Late, D. J.; Liu, B.; Matte, H. S. S. R.; Dravid, V. P.; Rao, C. N. R. Hysteresis in Single-Layer MoS_2 Field Effect Transistors. *ACS Nano* **2012**, *6*, 5635−5641.

(24) Late, D. J.; Huang, Y.; Liu, B.; Acharya, J.; Shirodkar, S. N.; Luo, J.; Yan, A.; Charles, D.; Waghmare, U. B. N.; Dravid, V. P.; Rao, C. N. R. Sensing Behavior of Atomically Thin-Layered MoS_2 Transistors. *ACS Nano* **2013**, *7*, 4879−4891.
(25) Kashid, R. V.; Late, D. J.; Chou, S. S.; Huang, Y. K.; De, M.; Joag, D. S.; More, M. A.; Dravid, V. P. Enhanced Field-Emission Behavior of Layered MoS_2 Sheets. *Small* **2013**, *9*, 2730−2734.
(26) Coleman, J. N.; Lotya, M.; Neill, A.; Bergin, S. D.; King, P. J.; Khan, U.; Young, K.; Gaucher, A.; De, S.; Smith, R.; Shvets, I. V.; Arora, S. K.; Stanton, G.; Kim, H.; Lee, K.; Kim, G. T.; Duesberg, G. S.; Hallam, T.; Boland, J. J.; Wang, J. J.; Donegan, J. F.; Grunlan, J. C.; Moriarty, G.; Shmeliov, A.; Nicholls, R. J.; Perkins, J. M.; Grieveson, E. M.; Theuwissen, K.; McComb, D. W.; Nellist, P. D.; Nicolosi, V. Two Dimensional Nanosheets Produced by Liquid Exfoliation of Layered Materials. *Science* **2011**, *331*, 568−571.
(27) Ratha, S.; Rout, C. S. Supercapacitor Electrodes Based on Layered Tungsten Disulfide-Reduced Graphene Oxide Hybrids Synthesized by a Facile Hydrothermal Method. *ACS Appl. Mater. Interfaces* **2013**, *5*, 11427−11433.
(28) Late, D. J.; Shirodkar, S. N.; Waghmare, U. V.; Dravid, V. P.; Rao, C. N. R. Thermal Expansion, Anharmonicity and Temperature Dependent Raman Spectra of Single- and Few-Layer $MoSe_2$ and WSe_2. *Chem. Phys. Chem.* **2014**, *15*, 1592−1598.
(29) Thripuranthaka, M.; Late, D. J. Temperature Dependence Phonon Shifts in Single-Layer WS_2. *ACS Appl. Mater. Interfaces* **2014**, *6*, 1158−1163.
(30) Thripuranthaka, M.; Kashid, R. V.; Rout, C. S.; Late, D. J. Temperature Dependent Raman Spectroscopy of Chemically Derived Few Layer MoS_2 and WS_2 Nanosheets. *Appl. Phys. Lett.* **2014**, *104*, 081911.
(31) Voiry, D.; Yamaguchi, H.; Li, J.; Silva, R.; Alves, D. C. B.; Fujita, T.; Chen, M.; Asefa, T.; Shenoy, V. B.; Eda, G.; Chhowalla, M. Enhanced Catalytic Activity in Strained Chemically Exfoliated WS_2 Nanosheets for Hydrogen Evolution. *Nat. Mater.* **2013**, *12*, 850−855.
(32) Late, D. J.; Liu, B.; Luo, J.; Yan, A.; Matte, H. S. S. R.; Grayson, M.; Rao, C. N. R.; Dravid, V. P. GaS and GaSe Ultrathin Layer Transistors. *Adv. Mater.* **2012**, *24*, 3549−3554.
(33) Ross, J.; Wu, S.; Yu, S.; Ghimire, H.; Jones, N. J.; Aivazian, A. M.; Yan, G.; Mandrus, J.; Xiao, D. G.; Yao, D.; Xu, W. X. Electrical Control of Neutral and Charged Exciton in a Monolayer Semiconductor. *Nat. Commun.* **2013**, *4*, 1474.
(34) Larentis, S.; Fallahazad, B.; Tutuc, E. Field Effect Transistors and Intrinsic Mobility in Ultra Thin $MoSe_2$ Layers. *Appl. Phys. Lett.* **2012**, *101*, 223104.
(35) Fang, H.; Chuang, S.; Chang, T. C.; Takei, K.; Takahashi, T.; Javey, A. High Performance Single Layered WSe_2 p-FETs with Chemically Doped Contacts. *Nano Lett.* **2012**, *12*, 3788.
(36) Liu, W.; Kang, J.; Sarkar, D.; Khatami, Y.; Jena, D.; Banerjee, K. Role of Metal Contacts in Designing High-Performance Monolayer n-Type WSe_2 Field Effect Transistors. *Nano Lett.* **2013**, *13*, 1983−1990.
(37) Potoczek, M.; Przybylski, K.; Rekas, M. Defect Structure and Electrical Properties of Molybdenum Disulphide. *J. Phys. Chem. Solids* **2006**, *67*, 2528−2535.
(38) Walek, S. D.; Donley, M. S.; Zabinski, J. S.; Dyhouse, V. J. Characterization of Pulsed Laser Deposited MoS_2 by Transmission Electron Microscopy. *J. Mater. Res.* **1993**, *8*, 2933.
(39) Chrisey, D. B.; Hubler, G. K. *Pulsed Laser Deposition of Thin Films*, 2nd ed.;John Wiley and Sons, Inc.: Hoboken, NJ, 2007.
(40) Singh, R. K.; Narayan, J. Pulsed Laser Evaporation Technique for Deposition of Thin Films: Physics and Theoretical Model. *Phys. Rev. B* **1990**, *41*, 8843.
(41) Singh, R. K.; Holland, O. W.; Narayan, J. Theoretical Model for Deposition of Superconducting Thin Films Using Pulsed Laser Evaporation Technique. *J. Appl. Phys.* **1990**, *68*, 233−247.
(42) Mattox, D. M.; Cuthrell, R. E.; Peeples, C. R.; Dreike, P. L. Preparation of Thick Stress Free Molybdenum Films for a Resistively Heated Ion Source. *Surf. Coat. Technol.* **1988**, *36*, 177−124.
(43) Donnet, C.; Mogne, T. L.; Martin, J. M. Superlow Friction of Oxygen Free MoS_2 Coatings in Ultrahigh Vacuum. *Surf. Coat. Technol.* **1993**, *62*, 406−411.
(44) Walck, S. D.; Zabinski, J. S.; Donley, M. S.; Bultman, J. E. Evolution of Surface Topography in Pulsed Laser Deposited Thin Films of MoS_2. *Surf. Coat. Technol.* **1993**, *62*, 412−416.
(45) Conley, H. J.; Wang, B.; Ziegler, J. I.; Haglund, R. F.; Pantelides, S. T.; Bolotin, K. I. Bandgap Engineering of Strained Monolayer and Bilayer MoS_2. *Nano Lett.* **2013**, *13*, 3626−3630.
(46) Luo, X.; Zhao, Y.; Zhang, J.; Xiong, Q.; Quek, S. Y. Anomalous Frequency Trends in MoS_2 Thin Films Attributed to Surface Effects. *Phys. Rev. B* **2013**, *88*, 075320.
(47) Yan, R.; Simpson, J. R.; Bertolazzi, S.; Brivio, J.; Watson, M.; Wu, X.; Kis, A.; Luo, T.; Walker, A. R. H.; Xing, H. G. Thermal Conductivity of Monolayer Molybdenum Disulfide Obtained from Temperature-Dependent Raman Spectroscopy. *ACS Nano* **2014**, *8*, 986−993.
(48) Fowler, R. H.; Nordheim, L. Electron Emission in Intense Electric Fields. *Proc. R. Soc. London* **1928**, *119*, 173.
(49) Forbes, R. G. Recent Developments in the Theory of Cold Field Electron Emission. *J. Appl. Phys.* **2008**, *103*, 114911.
(50) Forbes, R. G. Extraction of Emission Parameters for Large Area Field Emitters, Using a Technically Complete Fowler−Nordheim Type Equation. *Nanotechnology* **2012**, *23*, 095706.
(51) Walia, S.; Balendhran, S.; Wang, Y.; Kadir, R. A.; Zoolfakar, A. S.; Atkin, P.; Ou, J. Z.; Sriram, S.; Kalantar-zadeh, K.; Bhaskaran, M. Characterization of Metal Contacts for Two Dimensional MoS_2 Nanoflakes. *Appl. Phys. Lett.* **2013**, *103*, 232105.
(52) Yun, J.; Noh, Y.; Yeo, J.; Go, Y.; Na, S.; Jeong, H.; Kim, J.; Lee, S.; Kim; Koo, H. Y.; Kim, T.; Kim, D. Efficient Work Function Engineering of Solution Processed MoS_2 Thin Films For Novel Hole and Electron Transport Layers Leading to High Performance Polymer Solar Cell. *J. Mater. Chem. C* **2013**, *1*, 3777−3783.
(53) Yang, L.; Wang, S.; Zeng, Q.; Zhang, Z.; Peng, L. M. Carbon Nanotube Photoelectronic and Photovoltaic Devices and Their Applications in Infrared Detection. *Small* **2013**, *9*, 1225−1236.